

## Cu–Ni–PGE MINERALIZATION IN THE GENINA GHARBIA MAFIC–ULTRAMAFIC INTRUSION, EASTERN DESERT, EGYPT

HASSAN M. HELMY<sup>§</sup>

*Department of Geology, Minia University, 61111-Minia, Egypt*

### ABSTRACT

The Genina Gharbia intrusion is a small late Precambrian mafic–ultramafic complex in the Eastern Desert of Egypt. It comprises harzburgite, lherzolite, pyroxenite, norite and gabbro. The intrusion is not metamorphosed, but highly affected by faulting and shearing, and most of the original contacts have been obliterated. The various rocks are characterized by high modal content of magnesiohornblende and abundant phlogopite and fluorapatite. The Cu–Ni ore forms either disseminations in peridotite or massive patches in gabbro and consists of pyrrhotite >> pentlandite = chalcopyrite >> pyrite = violarite = cubanite and minor cobaltite–gersdorffite, nickeline, sphalerite, molybdenite and valleriite. Intense alteration commonly is associated with sulfides in gabbroic rocks, in which the silicate assemblage is dominated by actinolite, chlorite, epidote, albite and quartz. Platinum-group minerals (PGM) are restricted to bismuthotellurides of Pd, *i.e.*, michenerite and the melonite–merenskyite series; no Pt minerals were identified. The PGM are usually associated with hessite, altaite, tsumoite, sylvanite and native tellurium. Ninety percent of the PGM and other tellurides grains are located at sulfide–silicate contacts and as inclusions in altered silicates. The total Cu + Ni locally reaches up to 1.5 wt%, with a Cu:Ni ratio <1. Platinum-group elements (PGE) concentrations (maximum 260 ppb Pd, 65 ppb Pt, 9 ppb Rh, 38 ppb Ir, 10 ppb Ru, 7 ppb Os) were determined in sulfide-bearing samples. The Pd:Pt ratio increases from the hornblende harzburgite to hornblende gabbro. The mineralogical and chemical characteristics of the Genina Gharbia mineralization are best explained by a three-stage process: (1) a stage of magmatic crystallization in which the base metals and precious metals were concentrated in a sulfide melt largely in the harzburgite and lherzolite, (2) a late-magmatic stage in which base metals and precious metals were concentrated in a volatile-rich fluid, and (3) a postmagmatic stage of faulting and shearing, which locally remobilized metals and concentrated them along shear zones. In stage (1), the PGE were hosted in base-metal sulfides, mainly pentlandite and cobaltite–gersdorffite. The availability of semimetals (Te, Bi) in the late-magmatic fluid controlled the deposition of PGM in stage (2).

*Keywords:* platinum-group minerals, tellurides, genesis, Genina Gharbia, Egypt.

### SOMMAIRE

Le petit massif intrusif mafique–ultramafique de Genina Gharbia, d'âge précambrien tardif, est situé dans le désert oriental d'Égypte. Il contient harzburgite, lherzolite, pyroxénite, norite et gabbro. L'intrusion n'est pas métamorphosée, mais elle est fortement affectée par des cisaillements et des failles, de sorte que la plupart des contacts originels ont été oblitérés. Les diverses roches contiennent des proportions importantes de magnésiohornblende et une abondance de phlogopite et fluorapatite. Le minerai Cu–Ni soit des disséminations dans la péridotite ou bien des taches de minerai massif dans le gabbro, contenant pyrrhotite >> pentlandite = chalcopyrite >> pyrite = violarite = cubanite, avec des quantités moindres de cobaltite–gersdorffite, nickeline, sphalérite, molybdénite et valleriite. Une altération intense est généralement associée aux sulfures des roches gabbroïques, dans lesquelles l'assemblage de silicates contient surtout actinolite, chlorite, épidote, albite et quartz. Les minéraux du groupe du platine (MGP) sont uniquement des bismuthotellurures de Pd, par exemple michenerite et la série melonite–merenskyite; aucun minéral à dominance de Pt n'a été trouvé. Ces minéraux sont généralement associés à hessite, altaïte, tsumoïte, sylvanite et tellurium natif. Quatre-vingt-dix pour cent des grains de MGP et d'autres tellurures sont situés aux contacts entre sulfures et silicates, et sous forme d'inclusions dans les silicates formés lors de l'altération. La teneur totale en Cu + Ni atteint localement 1.5% (poids), avec un rapport Cu:Ni <1. La concentration des éléments du groupe du platine (EGP; maximum 260 ppb Pd, 65 ppb Pt, 9 ppb Rh, 38 ppb Ir, 10 ppb Ru, 7 ppb Os) a été déterminée dans les échantillons porteurs de sulfures. Le rapport Pd:Pt augmente de harzburgite à hornblende à gabbro à hornblende. Les caractéristiques minéralogiques et géochimiques de la minéralisation à Genina Gharbia semblent indiquer un processus à trois stades: (1) un stade de cristallisation magmatique au cours duquel les métaux de base et les métaux précieux se sont vus concentrés dans un bain fondu sulfuré, surtout dans les harzburgites et les lherzolites, (2) un stade tardi-magmatique au cours duquel les métaux de base et les métaux précieux se sont vus concentrés dans une phase fluide, et (3) un stade postmagmatique de déformation par failles et cisaillements, menant à une

<sup>§</sup> *E-mail address:* hmhelmy@yahoo.com

remobilisation locale des métaux et une concentration le long de zones de cisaillement. Au stade (1), les EGP étaient situés dans des sulfures de métaux de base, surtout pentlandite et cobaltite–gersdorffite. La disponibilité des semimétaux (Te, Bi) dans la phase fluide tardi-magmatique a exercé un contrôle important de la déposition des MGP au stade (2).

*Mots-clés:* minéraux du groupe du platine, tellurures, genèse, Genina Gharbia, Egypte.

## INTRODUCTION

In the course of exploration of basement rocks in the context of the United Nations Development Program (UNDP) of the Aswan Quadrangle, two small occurrences of Cu–Ni mineralization were found in 1973 (Bugrov 1974): Gabbro Akarem and Genina Gharbia. An extensive program of exploration was conducted in the two areas, and the occurrences were found to be uneconomic. Gabbro Akarem is now considered to be a Precambrian analogue of an Alaskan-type complex (Helmy & Mogessie 2001, Helmy & El Mahallawi 2003). The Cu–Ni–PGE mineralization at Gabbro Akarem is hosted mainly in ultramafic dunite pipes and shows a typical magmatic mineralogy and textures. Three platinum-group minerals (merenskyite, michenerite, palladoan bismuthian melonite) were documented (Helmy & Mogessie 2001). The consistently low PGE contents ( $\Sigma$ PGE <270 ppb) and their uniform distribution in sulfide-bearing and barren rocks were attributed to rapid crystallization of sulfides in a highly dynamic environment.

Since the discovery of the Genina Gharbia Cu–Ni prospect, very few studies have been carried out (Fredriksson 1974, Missak 1981, Kamel *et al.* 1990). In the area, disseminated and massive Cu–Ni sulfide ore is hosted in mafic–ultramafic rocks of Precambrian age. Geological, geochemical and geophysical studies carried out by the project geologists led to the location of two promising areas for detailed exploration work. The mineralization was traced on the surface, and four exploratory drillholes were put down, with a total of 621 m. Ore reserves were estimated at 270,000 tonnes (Fredriksson 1974). No mining activities have been done so far. Relevant studies of the geology and petrology of the Genina Gharbia rocks and sulfide mineralization include those by Fredriksson (1974), Khudier (1995), Missak (1981), Kamel *et al.* (1990), and El Mahallawi (1996).

In this contribution, I report the first occurrence of platinum-group minerals (PGM) and other tellurides at Genina Gharbia, describe the textural relations and chemical compositions of the various phases, present the first geochemical data on PGE contents, and discuss the genetic aspects. The type of PGM assemblage and associated tellurides reflects complicated late magmatic and postmagmatic hydrothermal processes. A summary of silicate mineralogy and mineral chemistry is also presented to support the proposed genetic model.

## GEOLOGICAL BACKGROUND

The Genina Gharbia intrusion is located in an area 175 km east of Aswan town (Fig. 1) in the south Eastern Desert of Egypt (Lat. 23°57' N, Long. 34°35'). This region is underlain by a late Proterozoic Shield cropping out east of the River Nile, and includes widespread exposures of mafic to intermediate metavolcanic rocks, immature sedimentary rocks, and abundant ultramafic rocks (El Gaby *et al.* 1990). Mafic–ultramafic units are either tectonically emplaced ophiolitic or magmatic intrusions (Takla & Noweir 1980). The Genina Gharbia area is one of many magmatic intrusions located along deep structures that intersect the basement in an east–northeasterly direction (Helmy & El Mahallawi 2003).

The Genina Gharbia mafic–ultramafic intrusion covers an area 9 km long and 3.5 km wide and comprises harzburgite, lherzolite, pyroxenite and various types of gabbro; all are hornblende-bearing. The age of the intrusion is not known, but the intrusive relation with other rocks (calc-alkaline granites) in the area suggests a late Precambrian age. Two large and many small harzburgite–lherzolite bodies are found in the area as low hills located in valleys. The largest bodies (1–2 km in diameter), found in the southeastern part of the area (Fig. 2), have gradational contacts with the surrounding pyroxenite, whereas small bodies (100–300 m in diameter), dominant in the northwestern part, have tectonic contacts against the surrounding rocks. Although the Cu–Ni sulfide ore is recorded in both large and small ultramafic bodies, the mode of occurrence of sulfides differs from one to the other (see below).

Pyroxenite commonly forms small bodies bounded by faults in the northwestern part of the area, whereas zones of this rock are found in contact with the larger bodies of harzburgite and lherzolite. This rock shows variable degrees of alteration.

Norite, also variably altered, forms high hills surrounding the ultramafic rocks, and covers the outer parts of the intrusion. Gradational contacts with the ultramafic rocks are characteristic (El Mahallawi 1996). Norite close to granitic rocks is more altered relative to that in contact with the ultramafic rocks (Khudier 1995).

Khudier (1995) demonstrated that the different rock units were derived from a tholeiitic magma by fractional crystallization. On the basis of rare-earth-element (REE) data, El Mahallawi (1996) suggested that the parental magma was derived from a contaminated source that experienced subduction.

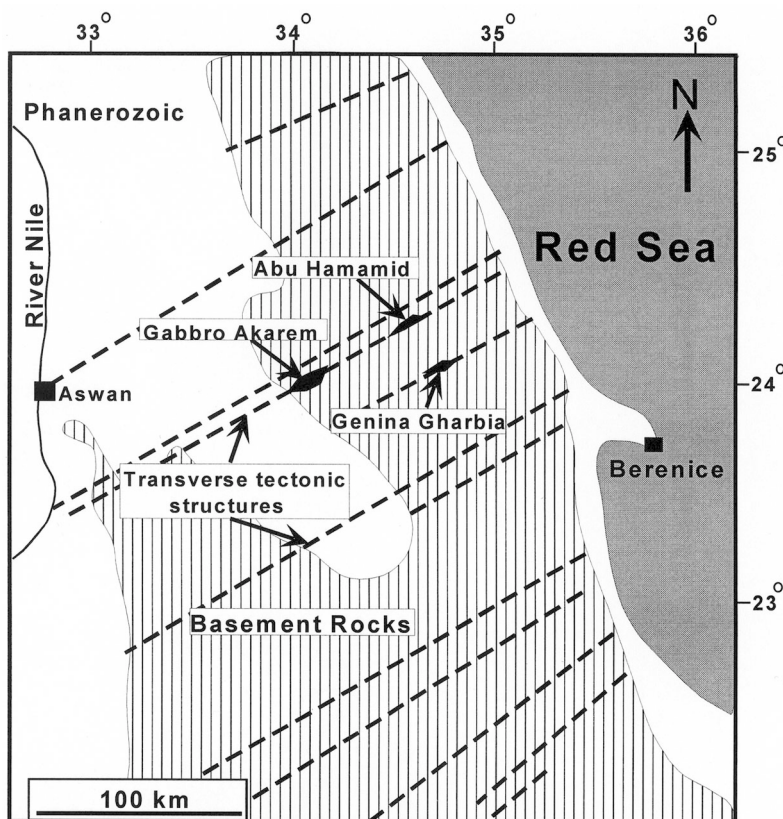


FIG. 1. Location map of the Genina Gharbia area and other concentrically zoned complexes in the Eastern Desert of Egypt (Helmy & El Mahallawi 2003).

#### STRUCTURES

The Genina Gharbia intrusion is gently folded, with a plunging fold axis trending N 20°E (Fredriksson 1974). Despite this fold, the area is structurally simple, except in the northwestern part (Fig. 2), where two major fault systems intersect, an older WNW-trending set and younger NNW-trending faults. The former faults commonly have a strike-slip component.

Figure 3 is a detailed geological map of the northwestern part of the area. Many faults and small shear-zones are recognized; all geological contacts have been obliterated by tectonism. On the surface, shear zones are in some cases marked by gossans, which are traceable for more than 200 meters. In the drill core, faults are marked by the abrupt change in lithology and slickensides, whereas shear zones are marked by an extensive alteration of the silicate assemblage. The sulfide mineralization is concentrated in this highly tectonized part of the area (Figs. 2, 3).

#### GEOLOGY OF THE MINERALIZED AREA

The northwestern part of the area, close to the metasedimentary rocks, is highly dissected by faults (Fig. 3). Various rock types are recognized on the surface, *i.e.*, harzburgite, lherzolite, pyroxenites, norite and gabbros and metasedimentary rocks, and sudden changes in rock type are a common feature. In this part, gossans form long zones extending for tens of meters. Quartz veins have been observed in the northern part close to the metasedimentary rocks. This area was selected for detailed geological, geophysical and geochemical work (Bugrov 1974). Geochemical prospecting by the UNDP geologists pointed to anomalous values of Cu and Ni along a line of thin gossans. A reconnaissance magnetometric survey of the area underlain by peridotite (harzburgite and lherzolite) led to the detection of two strong positive anomalies coincident with the pyroxenite-peridotite contacts (Guillon 1974). Four cores were drilled in the area showing geochemi-

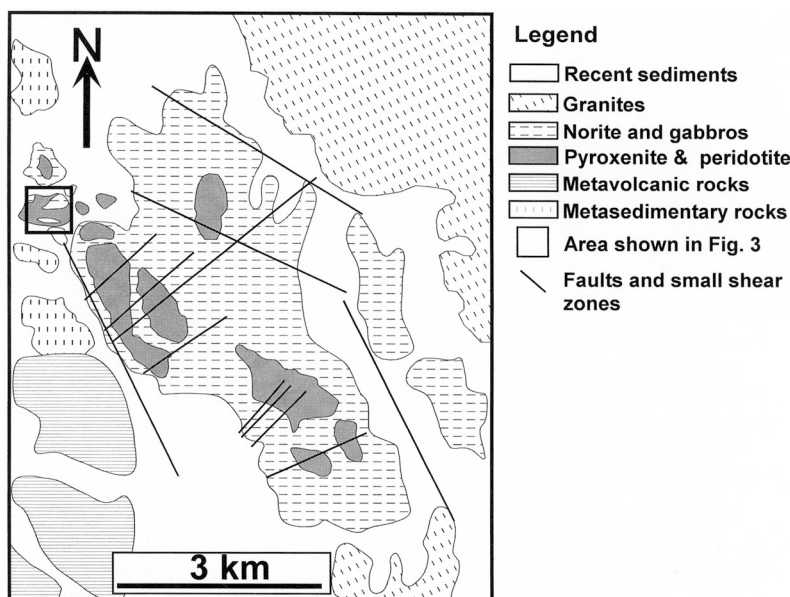


FIG. 2. Geological map of the Genina Gharbia area (after Fredricksson 1974, with modifications).

cal anomalies (Bugrov 1974); DH 1, 2, 3 and 4. DH1 was drilled with an inclination of  $50^\circ$  (azimuth  $290^\circ$ ) to a depth of 150 m. The other three cores were located on one southeastern profile (Fig. 3); all the three cores were made perpendicular to the dip of the gossan zone. DH2 was located 30 m to the southeast of the gossan zone with an inclination of  $50^\circ$  (azimuth  $319^\circ$ ) to a depth of 30 m. DH3 and 4 (placed 50 and 110 m to the southeast of DH2, respectively) were drilled with an inclination of  $60^\circ$  to a depth of 160 and 281, respectively. Detailed petrographic studies of the cores (Fredriksson 1974, Missak 1981) proved that the mafic-ultramafic rocks contain disseminated, and locally massive, sulfide ore.

Important geological and petrographic observations can be deduced from the four cores (Fig. 4): 1) Two types of contacts are observed; primary (gradational) and tectonic contacts. The gradational contacts are observed within the same rock unit, *e.g.*, ultramafic rocks, where different modal compositions reflect primary magmatic layering. The tectonic contacts are marked by the abrupt change in rock type repeated over short intervals within the core and by gossans on surface. This abrupt change in lithology is consistent with the structural complexity of the site. 2) Many faults and shear zones are recognized in the core; extensive alteration and variable sulfide textures characterize these zones.

#### ANALYTICAL TECHNIQUES

Samples for this study were collected from surface exposures from the northwestern part of the intrusion and from core DH4, archived at the Geological Survey of Egypt. Petrographic studies as well as analyses of silicate, sulfide and platinum-group minerals (PGM) were performed on 28 polished thin sections. Electron-microprobe analyses were made using a JEOL JSM-6310 instrument with attached energy-dispersion system (EDX) and Microspec wavelength-dispersion system (WDX) at the Institute of Mineralogy and Petrology, Karl Franzens University, Graz, Austria. The accelerating voltage was 20 keV for the analysis of sulfides and PGM, and 15 keV for silicates at a probe current of 5 nA. The silicate standards were K-feldspar for Si, K and Al, garnet for Fe, Mg and Mn, titanite for Ca and Ti, chromite for Cr, and jadeite for Na. Standards for sulfides and PGM were chalcopyrite for Cu, pyrite for S and Fe, pure Ni and Co, tellurobismuthite ( $\text{Bi}_2\text{Te}_3$ ) for Bi and Te, PdS for Pd, sperrylite ( $\text{PtAs}_2$ ) for Pt, calaverite ( $\text{AuTe}_2$ ) for Au and pure silver. Nineteen samples were analyzed for PGE and Au by ICP-MS (nickel sulfide digest). The contents of Ag, Ni, Co, and Cu were measured by flame atomic absorption spectrometry (triple acid digest) and for S by inductively coupled plasma – optical emission spectrometry (ICP-

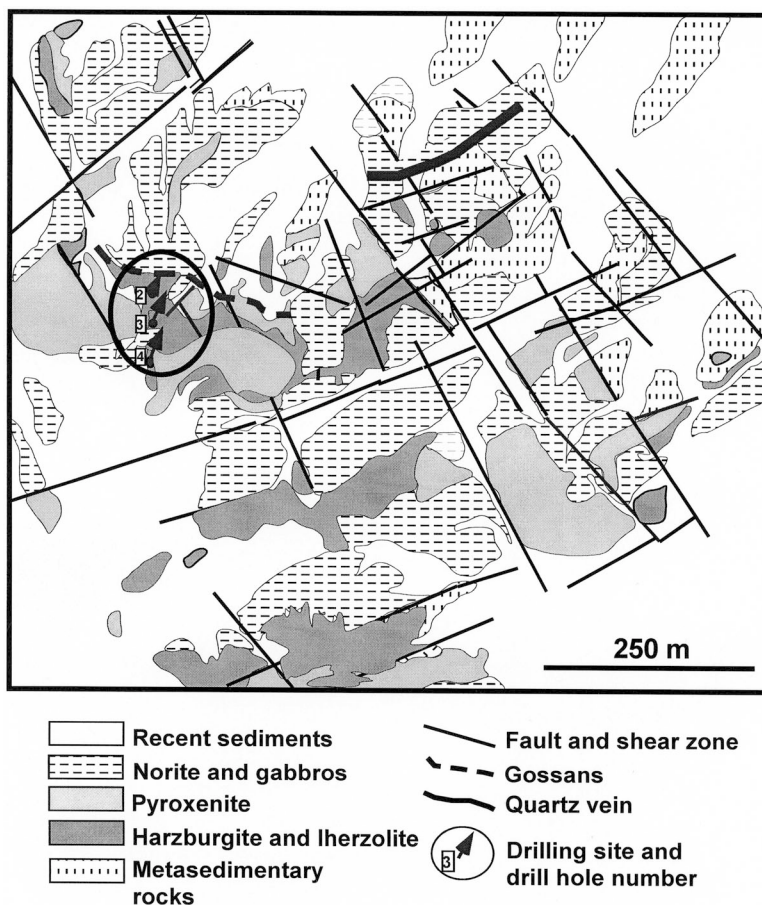


FIG. 3. Detailed geological map of the mineralized portion of Genina Gharbia intrusion, indicating drill-core sites.

OES) (triple acid digest) by Genalysis, Australia and Actlabs, Canada. The detection limit of PGE was 2 ppb for Ir, Os, and Ru, and 1 ppb for Pt, Pd and Rh.

#### PETROGRAPHY AND MINERAL CHEMISTRY

Core samples demonstrate that the Genina Gharbia intrusion consists of alternating units of harzburgite, lherzolite, pyroxenite and gabbro. There is no regular variation of lithology in the same core and between different ones, *i.e.*, individual rock units cannot be correlated between cores. The gabbros form the basal units of cores 1, 2 and 3 and the upper section of core 4, whereas ultramafic rocks (harzburgite and lherzolite) form the upper section of cores 1 and 3. Quartz diorite was observed over a narrow interval in core 4. The following paragraphs provide a petrographic description of the rock units. For the purposes of this study, alter-

ation of the various rocks is discussed in a separate section.

#### *The ultramafic rocks*

The ultramafic rocks in the Genina Gharbia area are represented by harzburgite, lherzolite, and pyroxenite, in order of decreasing abundance. The rocks represent a complete sequence of cumulates; all are hornblende-bearing and variably altered.

Harzburgite was observed in three cores (Fig. 4). It is coarse-grained and formed of olivine (50–70% modal), enstatite (20–30%), magnesiohornblende (5–15%), minor diopside and sulfides, and traces of a chromian spinel. Whereas most samples are fresh or partly altered, some samples are completely altered to serpentinite. Olivine (Fo<sub>81–85</sub>) forms large crystals (2–4 mm in diameter) as an early-crystallized cumulus phase,

followed by enstatite and magnesiohornblende. The latter form large interstitial grains enclosing olivine and chromian spinel (Fig. 5A). Chromian spinel commonly occurs as small (<100  $\mu\text{m}$ ) grains included in olivine, enstatite and magnesiohornblende, and also as an intercumulus phase (Fig. 6A). Sulfide-bearing samples contain up to 20% sulfides, which occur as intercumulus grains.

The lherzolite is petrographically similar, but with a higher modal contents of diopside (>15%) and magnesiohornblende (10–15%). The rock is coarse-grained and shows variable degrees of alteration, even within the same thin section.

Pyroxenite contains mainly enstatite (up to 40%), diopside (up to 25%), magnesiohornblende (up to 30%),

olivine (up to 12%) and plagioclase (up to 8%). Phlogopite, fluorapatite and chromian spinel are minor components. Enstatite ( $\text{En}_{79-81}$ ) and magnesiohornblende ( $\text{Mg\# 87-93}$ ) form large crystals apparently in equilibrium with olivine ( $\text{Fo}_{81-82}$ ). Plagioclase occurs as large unzoned crystals. Phlogopite forms large crystals interstitial to other phases and commonly coexists with fluorapatite grains (Fig. 5B). Fluorapatite occurs as large (200  $\mu\text{m}$ ) grains interstitial to early-formed silicates (Fig. 5C). Phlogopite and fluorapatite contain up to 1.2 and 2.5% Cl, respectively (Table 1). Textural observations suggest that the crystallization path of anhydrous and hydrous minerals (listed in order of first appearance) is chromian spinel, olivine, plagioclase, pyroxenes, magnesiohornblende and phlogopite.

#### Mafic rocks

Mafic rocks are represented by hornblende-bearing norite and gabbro. Quartz diorite was located over a short depth-interval between 150 and 160 m in core 4, and on the surface, it occurs as dykes intersecting the gabbros. These rocks also show variable degrees of alteration.

Norite consists of enstatite ( $\text{En}_{70-75}$ ), plagioclase, diopside, tschermakite and magnesiohornblende ( $\text{Mg\# 83-88}$ ), olivine and phlogopite as primary minerals. Ilmenite is the most common opaque mineral. Gabbro is made up of plagioclase (up to 60%), enstatite (10–20%) and minor hornblende. This rock is sulfide-bearing and extensively altered, and now contains secondary actinolite, epidote, albite and quartz. The quartz diorite dyke is a fine-grained rock composed mainly of plagioclase, hornblende with subordinate amounts of albite and quartz. Representative results of electron-microprobe analyses of phlogopite, fluorapatite and other accessory phases are reported in Table 1.

#### Alteration

The majority of mafic and ultramafic rock samples are fresh or weakly altered. A higher degree of alteration characterizes the mineralized gabbroic rocks and some of the unmineralized ultramafic rocks along shear zones. Here, talc–magnesite rock is well developed, especially along slickensides. Strong alteration is not preferentially associated with the presence of sulfides, especially in the ultramafic rocks. The weak alteration of ultramafic rocks is manifested by the replacement of olivine by serpentine (Figs. 5A, B). Plagioclase does not show any signs of alteration in these weakly altered rocks.

Along shear zones, the ultramafic rocks are intensely altered. Olivine and the pyroxenes are largely altered to serpentine, chlorite, talc–magnesite and iron oxides, which form small veinlets. Sulfides, where present, are replaced by magnetite.

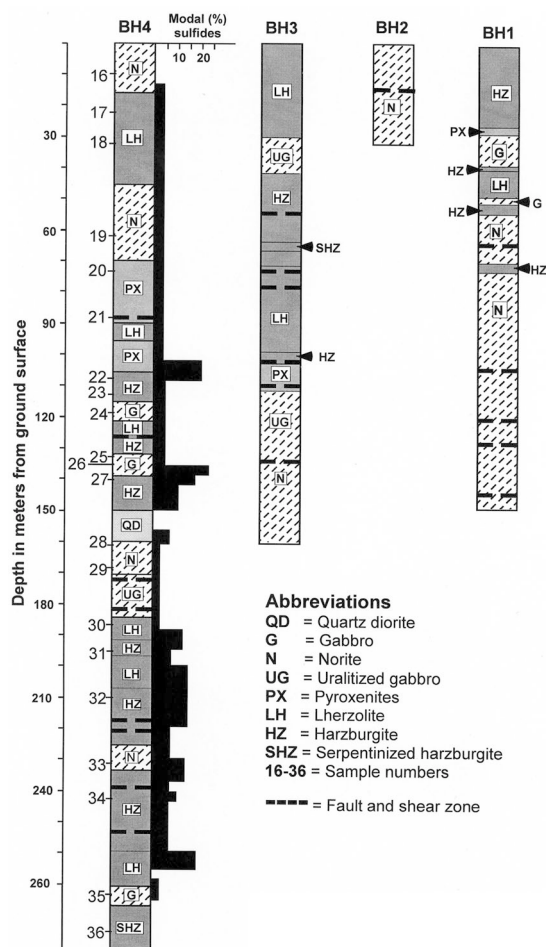


FIG. 4. Lithologies of the core samples from the Genia Gharbia intrusion indicating sample locations. Sample numbers have an G prefix in the text and tables.

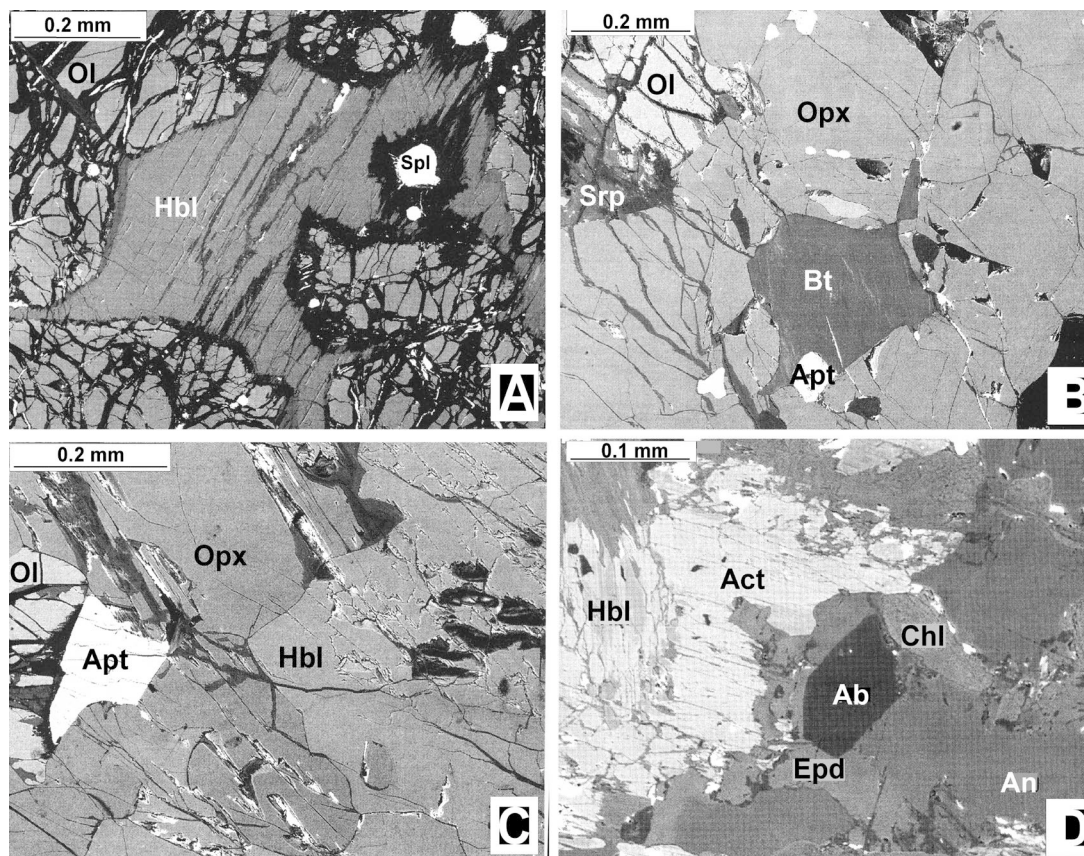


FIG. 5. Back-scattered images showing different textures of silicates. A) Intercumulus hornblende (Hbl) between cumulus olivine (Ol) crystals partially altered to serpentine (black), harzburgite, sample GG31. B) Olivine (Ol) partially altered to serpentine (Srp), biotite (Bt) with apatite (Apt) interstitial to orthopyroxene (Opx), pyroxenite, sample GG22. C) Large apatite (Apt) in direct contact with partially serpentinized olivine, orthopyroxene (Opx) and primary hornblende (Hbl), pyroxenite, sample GG22. D) Secondary actinolite (Act) and chlorite replacing hornblende and epidote (Epd) and albite (Ab) after anorthite (An), gabbro, sample GG25.

In the mineralized gabbroic rocks, intense alteration is common. The pyroxenes are replaced by actinolite–tremolite and chlorite, and plagioclase by epidote and quartz (Fig. 5D). Epidote commonly develops at the sulfide–actinolite contacts. Close to the patches of sulfide, only secondary silicates, *i.e.*, quartz, actinolite, albite, epidote and chlorite are present. Most of the massive sulfide patches are completely surrounded by quartz. Platinum-group minerals are commonly hosted in these secondary silicates.

#### The Cu–Ni sulfide ore

Base-metal sulfides (pyrrhotite, pentlandite and chalcocopyrite) are observed in all rock units, but modal abundances vary. At the surface, weathered sulfides make

gossan zones up to 3 m thick traced for tens of meters. Although located mainly at the contact between peridotite and pyroxenite (Fig. 3), gossan is developed on any rock type. Norite is barren (only small chalcocopyrite and pyrrhotite grains scattered in the matrix silicates). The mineralized gabbros are usually altered and contain patches of massive sulfides, which may form up to 20 vol.% of the sample. In all ultramafic units, sulfides form at least 5%; this percentage increases in the harzburgite and lherzolite, but significantly decreases in the highly serpentinized rocks (Fig. 4).

Sulfides occur sporadically throughout the drill core. The modal abundance of sulfides in the upper hundred meters of the core does not exceed 3%. In the lower part of the core, the sulfide content varies between 5 and 20%; the higher concentration of sulfides is particularly

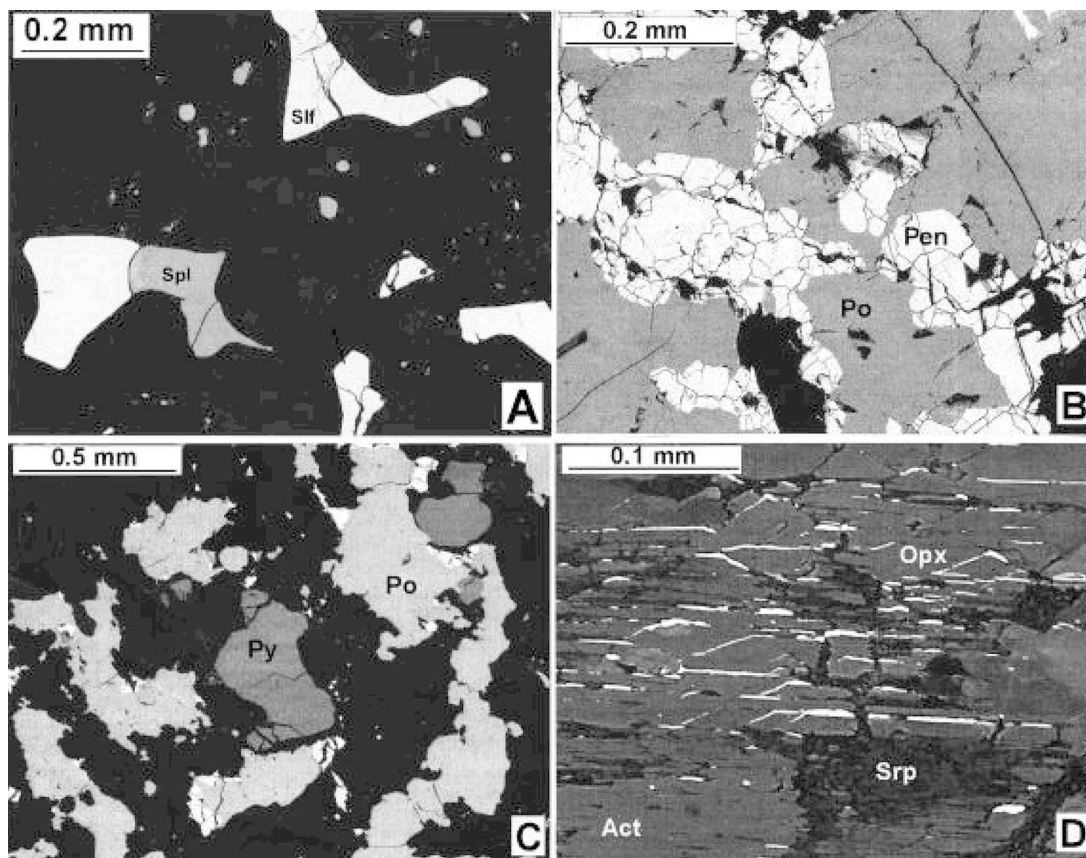


FIG. 6. Back-scattered images showing a variety of sulfide textures. A) Intercumulus sulfides (slf) and chromian magnetite (spl) in olivine and orthopyroxene (black) matrix. Notice the small rounded spinel grains included in silicates, lherzolite, sample GG18. B) Microveinlets of pentlandite (Pen) in pyrrhotite matrix (Po) making massive sulfide patch in sulfide-bearing gabbro, sample GG26. C) Anhedral pyrrhotite (Po) and pyrite (Py) in secondary silicate matrix (black), sulfide-bearing gabbro, sample GG24. D) Sulfides (white) along cleavage in orthopyroxene, which is partly altered to actinolite and serpentine, pyroxenite sample GG29.

noted in the ultramafic units. The distribution of sulfides within each rock unit is not regular; higher contents are observed along shear zones intersected by the core. Small patches of massive sulfides are encountered in the gabbros.

Various textures can be seen in the sulfide ore: 1) Disseminated sulfides, where the sulfides form small polymineralic globules included in, or interstitial to, the mafic silicates. This type is common in almost all rock units. 2) Network sulfide ore is observed in the mineralized samples from the undeformed harzburgite and lherzolite (Fig. 6A). 3) Massive patches, a few centimeters across, of sulfides in gabbro. Light-colored secondary silicates, *i.e.*, quartz, epidote and albite, invariably surround these patches. The boundaries of sulfides with the surrounding silicates are irregular (Fig. 6C). 4) Re-

placement sulfides, where sulfides occur along cleavage planes of enstatite (Fig. 6D). 5) Brecciated sulfides are observed along shear zones, the elongate grains being interstitial to chlorite, talc and magnesite (Fig. 7A).

The main sulfide minerals are pyrrhotite (40–50%), pentlandite (25–20%), chalcopyrite (20–25%), with lesser amounts of cubanite, violarite and pyrite and rare cobaltite, nickeline, molybdenite and sphalerite. The latter four minerals are described from the deposit for the first time.

Pyrrhotite is the most common sulfide at Genina Gharbia. In the disseminated sulfide ore, it forms small rounded grains. In the network and massive patches of sulfides, it occurs as relatively large granular grains without distinct cleavage. The mineral rarely forms monomineralic grains, being commonly intergrown

with chalcopyrite and pentlandite, and it carries flame-like lamellae of the latter. Laths of cubanite are also observed in pyrrhotite. The latter is the first phase to crystallize among the sulfide minerals. Replacement by magnetite is very common in the network sulfide ore. Electron-microprobe analyses (Table 2) reveal a metal:sulfur ratio of nearly (0.9 : 1.0) with Co contents ranging from 0.11 to 0.16 wt.%. Pyrrhotite from the gabbro contains higher Ni content (average 0.55 wt.%) relative to pyrrhotite from the harzburgite (average 0.22 wt.%).

Pentlandite is the second most abundant sulfide mineral; it forms massive veinlets (Fig. 6B) of idiomorphic grains and also lamellae within pyrrhotite. The mineral commonly contains blebs of mackinawite and is replaced by violarite, mostly in the hornblende gabbro. The chemical composition of the pentlandite (Table 2) varies only slightly within the same sample and rock

unit. A narrow range of Ni (31.17 to 33.36 wt.%) and Fe (31.1 to 32.1 wt.%) contents characterizes pentlandite from Genina Gharbia. The Ni/(Fe + Ni) value is between 0.49 and 0.51 in the ultramafic rocks, and between 0.479 and 0.484 in gabbro. Pentlandite from harzburgite contain more Co (2.0–2.76 wt.%) than that from gabbro (0.97–1.36 wt.%).

Chalcopyrite forms coarse-grained anhedral aggregates. It is concentrated close to the outer margin of pyrrhotite grains. Copper contents of chalcopyrite vary from 33.6 to 35.7 wt.%, the highest Cu contents (>35 wt.%) being recorded in chalcopyrite from the ultramafic rocks. Very low contents of Co and Ni (generally below 0.06%) are detected in chalcopyrite (the metal : sulfur ratio is 1 : 1).

Cubanite and isocubanite commonly form lath-like lamellae or massive rounded patches in chalcopyrite from the network and sheared sulfides in the ultramafic

TABLE 1. REPRESENTATIVE COMPOSITIONS OF SOME SILICATES AND APATITE FROM GENINA GHARBIA, EGYPT

Sample	GG20 Phl	GG21 Phl	GG24 Ab	GG26 An	GG24 An	GG25 Ttn	GG25 Ep	GG21 Ap	GG21 Ap	GG20 Ap
SiO <sub>2</sub> wt%	39.87	38.35	67.55	52.67	53.68	30.57	37.88	0.26	0.34	0.25
TiO <sub>2</sub>	0.59	0.53	—	—	—	40.08	0.14	0.02	n.d.	n.d.
Al <sub>2</sub> O <sub>3</sub>	16.82	16.32	20.14	30.66	30.11	0.47	25.43	0.29	0.15	0.13
Cr <sub>2</sub> O <sub>3</sub>	0.11	0.13	—	—	—	0.14	—	—	—	—
FeO	5.957	6.09	—	—	—	—	10.6	0.18	0.41	0.44
Fe <sub>2</sub> O <sub>3</sub>	—	—	0.09	0.19	0.17	0.28	—	—	—	—
MgO	22.79	22.61	—	—	—	0.05	0.11	0.23	0.16	0.16
CaO	0.21	—	0.97	12.49	12.41	27.25	23.55	52.91	53.49	53.78
Na <sub>2</sub> O	1.39	1.43	10.91	3.91	4.15	—	—	n.d.	n.d.	n.d.
K <sub>2</sub> O	7.28	7.42	0.13	0.09	0.1	—	—	n.d.	n.d.	n.d.
P <sub>2</sub> O <sub>5</sub>	—	—	—	—	—	—	—	39.97	40.64	40.51
Cl	1.52	0.46	—	—	—	—	—	2.49	0.89	0.71
F	2.2	2.63	—	—	—	0.27	—	3.2	2.3	2.9
Total	98.737	95.97	99.79	100.01	100.62	99.11	97.71	99.55	98.38	98.88
O	22	22	8	8	8	20	13	26	26	26
Si <i>apfu</i>	5.409	5.349	2.961	2.382	2.411	4.013	2.976	0.050	0.060	0.040
Ti	0.060	0.056	—	—	—	3.957	0.008	—	—	—
Al	2.689	2.682	1.041	1.634	1.594	0.073	2.355	0.060	0.030	0.030
Cr	0.012	0.014	—	—	—	0.015	—	—	—	—
Fe <sup>3+</sup>	0.608	0.639	—	—	—	—	0.627	—	—	—
Fe <sup>2+</sup>	—	—	0.003	0.007	0.006	0.031	—	0.030	0.060	0.040
Mg	4.608	4.700	—	—	—	0.010	0.013	0.060	0.040	0.040
Ca	0.031	—	0.046	0.605	0.597	3.833	1.982	10.320	10.290	10.350
Na	0.366	0.387	0.927	0.343	0.361	—	—	—	—	—
K	1.260	1.320	0.007	0.005	0.006	—	—	—	—	—
P	—	—	—	—	—	—	—	6.160	6.180	6.160
Cl	0.349	0.109	—	—	—	—	—	0.770	0.270	0.220
F	0.944	1.160	—	—	—	0.112	—	1.840	1.310	1.650
Σ cations	16.336	16.415	4.985	4.976	4.976	12.042	9.088	19.290	18.240	18.530
An mol.%	—	—	4.7	63.5	61.9	—	—	—	—	—
Ab	—	—	94.6	35.9	37.5	—	—	—	—	—
Fe <sup>3+</sup> /(Fe <sup>3+</sup> + Al)	—	—	—	—	—	—	0.21	—	—	—

n.d.: not detected, —: not measured. Symbols: Phl: phlogopite, Ap: apatite, Ab: albite, An: anorthite, Ttn: titanite, Ep: epidote. Representative results of electron-microprobe analyses.

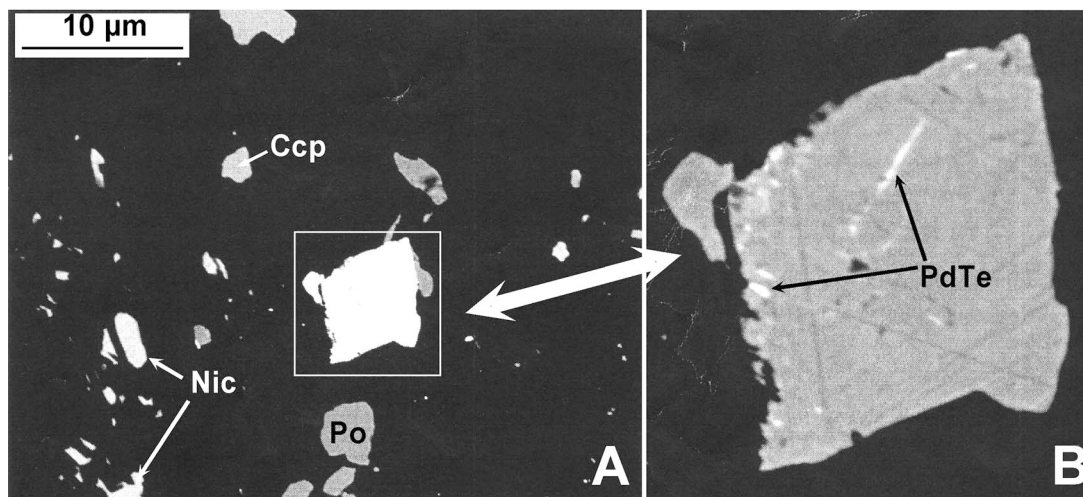


FIG. 7. A) Brecciated pyrrhotite (Po), chalcopyrite (Ccp), nickeline (Nic) and cobaltite (inside the square) in a secondary silicate matrix along a small shear-zone, harzburgite, sample GG23. B) The cobaltite grain (in A) containing fine exsolution-induced domains of a Pd-Te phase (PdTe).

TABLE 2. REPRESENTATIVE COMPOSITIONS OF SULFIDE MINERALS, GENINA GHARBIA, EGYPT

Sample	GG26 Po	GG27 Po	GG26 Py	GG32 Pn	GG29 Pn	GG22 Mkw	GG26 Cbn	GG23 Cbt	GG27 Cbt	GG23 Nc	GG25 Mlb
S wt%	39.62	39.18	52.63	33.62	33.92	39.41	35.01	19.89	18.15	2.52	32.28
Te						n.d.		n.d.	n.d.	n.d.	1.31
Fe	60.02	59.87	45.26	32.27	31.58	56.84	40.41	4.99	6.01	4.95	0.28
Cu	n.d.	n.d.	n.d.	n.d.	n.d.	n.d.	24.09	n.d.	n.d.	n.d.	n.d.
Ni	0.63	0.29	0.08	31.17	33.36	1.74	n.d.	6.52	8.92	39.52	0.21
Co	0.12	0.1	0.75	2.76	1.18	0.14	0.08	22.57	22.31	1.31	
Mo	—	—	—	—	—	—	—	—	—	—	64.51
As	—	—	—	—	—	—	—	44.21	42.76	51.31	0.21
Ag	—	—	—	—	—	—	—	n.d.	n.d.	n.d.	2.1
Pd	n.d.	n.d.	n.d.	n.d.	n.d.	n.d.	n.d.	1.84	1.25	n.d.	0.43
Pt	n.d.	n.d.	n.d.	n.d.	n.d.	n.d.	n.d.	0.06	0.51	n.d.	n.d.
Total	100.39	99.44	98.72	99.82	100.04	98.13	99.59	100.08	99.91	99.61	101.33

n.d.: not detected, —: not measured, Po: pyrrhotite, Py: pyrite, Pn: pentlandite, Cbn: cubanite or isocubanite, Mkw: mackinawite, Cbt: cobaltite, Nc: nickeline, Mlb: molybdenite. Representative results of electron-microprobe analyses.

rocks. The laths are invariably perpendicular to the boundaries of chalcopyrite grains. The patches of massive cubanite and isocubanite may host small grains of pentlandite, violarite and pyrrhotite. Cubanite is relatively Cu-rich (24–25 wt.%) and contains traces of Co (0.1–0.2 wt.%).

Pyrite is restricted to euhedral porphyroblasts within chalcopyrite and pyrrhotite, and is also developed as isolated grains in massive sulfides (Fig. 6C). It contains

relatively high Co (0.46 to 1.0%) and low Ni (<0.1%) contents.

Mackinawite occurs as small lamellae (up to 100 µm) in pentlandite. It forms about 10% of the pentlandite grains in the oxidized sulfides (replaced with magnetite). It was not observed in chalcopyrite. Mackinawite from Genina Gharbia is very poor in Cu (below the detection limit) and poor in nickel (1.1 to 1.74 wt.%) relative to mackinawite from the metamor-

phosed Abu Swayel Cu-Ni-PGE mineralization (Helmy *et al.* 1995). In the latter deposit, mackinawite is hosted in chalcopyrite and contains up to 4.6 and 6.0 wt.% Cu and Ni, respectively.

Molybdenite forms either single laths up to 200  $\mu\text{m}$  in size commonly included in the massive sulfide patches in hornblende gabbro, or short twinned crystals in the silicate matrix, which is made of epidote, actinolite and quartz. Electron-microprobe analyses of the mineral reveal two distinct compositions. The molybdenite included in secondary silicates contains low Mo (52.1–54.5 wt.%) and high S (37.3–38.8 wt.%) contents. This variety contains relatively high contents of Ag (1.7–5.0 wt.%), Te (1.2–3.7 wt.%), Fe (0.3–0.6 wt.%), Pd (0.4–0.5 wt.%) and Ni (0.2–0.3 wt.%). Such high contents of Ag, Te, Pd, and Ni have never been recorded in molybdenite from any similar deposit worldwide. Molybdenite included in sulfides contains high Mo (64–66 wt.%), low S (33.1–33.9 wt.%) contents and traces of Fe (<0.3 wt.%) and Ni (<0.2 wt.%). The concentrations of Ag, Te and Pd in this molybdenite are below the detection limit.

Cobaltite occurs as small (<80  $\mu\text{m}$ ) idiomorphic crystals included in pyrrhotite and as isolated grains in brecciated sulfides. Very fine lamellae of a PdTe phase have been noted in cobaltite (Fig. 7B). Large variations in the Co (from 18.8 to 25.2 wt.%) and Ni (from 6.0 to 10.5%) contents are characteristic. Relatively high contents of Pd (up to 1.84 wt.%) and Pt (up to 0.5 wt.%) were detected in cobaltite.

Nickeline forms small (<50  $\mu\text{m}$ ) bright grains in sheared ultramafic rocks (Fig. 7A). The mineral occurs

as isolated angular grains filling between the secondary silicates (mainly chlorite and talc). Nickeline has a narrow range of chemical composition (Table 2), with As and Ni contents ranging from 49.2 to 51.3 wt.% and from 39.5 to 42.5 wt.%, respectively. Relatively high contents of S (1.9–2.5 wt.%) and Co (1.1–1.3 wt.%) are detected in nickeline.

Sphalerite is the least-abundant sulfide mineral at Genina Gharbia. It forms small grains (<50  $\mu\text{m}$ ) intergrown with pyrrhotite and chalcopyrite. The content of Fe is high (6–8 wt.%), whereas Cd and Mn are low (both <0.2 wt.%).

Valeriite occurs as small veinlets along cracks in serpentinized olivine. In addition to magnetite replacing sulfides, thin veinlets of magnetite are developed along cracks in serpentinized olivine, together with valeriite.

#### GEOCHEMICAL DATA

The S, Cu, Ni, Co, Zn, Cr, As, Sb, Se, Mo and noble-metal concentrations in nineteen variably mineralized samples representing various rock units from drill core DH4 at Genina Gharbia are listed in Table 3.

#### Base metals

Although the sulfide-bearing (samples GG24, GG25 and GG26) gabbros and sulfide-poor (samples GG16, GG19 and GG28) samples of norite contain similar low contents of Cr (from 81 to 260 ppm and from 170 to 190 ppm, respectively), distinct differences in base-metal

TABLE 3. ANALYTICAL DATA ON THE GENINA GHARBIA SAMPLES

Sample	D	R	S	Cr	V	Cu	Ni	Co	As	Sb	Mo	Zn	Se	Ag	Pd	Pt	Rh	Au	Ir	Os	Ru	Pd/Pt	Cu/Ni/Pd/Ir	
GG16	10	N	0.12	81	52	22	121	42	0.5	0.1	2	42	1	0.4	<1	<1	<1	2	<2	<2	<2	1.00	0.18	—
GG17	23	L	0.74	3200	60	600	2620	190	<0.5	<0.1	<1	60	<1	<0.4	8	12	<1	4	<2	<2	<2	0.67	0.23	>4
GG18	33	L	1.5	2900	98	3040	5890	230	<0.5	<0.1	1	30	<1	<0.4	86	16	3	36	23	2	18	5.38	0.52	4
GG19	63	N	0.3	280	41	290	340	29	<0.5	<0.1	<1	32	<1	<0.4	3	<1	9	1	<2	<2	<2	>3	0.85	>1.5
GG20	88	P	0.14	2200	78	454	1141	120	1	0.2	2	95	3	0.9	<1	3	<1	84	<2	<2	<2	<0.3	0.40	—
GG21	105	P	1.5	1200	49	650	3500	170	<0.5	<0.1	<1	40	2	<0.4	12	<1	8	<1	<2	<2	<2	>12	0.19	>6
GG22	108	H	1.5	3400	90	2660	7220	280	1	<0.1	<1	27	2	<0.4	63	7	0	9	<2	<2	<2	9.00	0.37	>32
GG23	113	H	2.2	2100	50	3200	6800	270	<0.5	<0.1	<1	45	2	150	26	2	19	5	<2	10	5.77	0.47	30	
GG24	120	G	3.9	180	57	2312	8275	320	3	0.5	3	62	19	1	210	1	<1	11	<2	<2	210.00	0.28	>105	
GG25	136	G	3.8	170	55	2100	5100	130	5	0.3	4	57	18	1.4	226	3	6	8	<2	<2	3	75.33	0.41	>113
GG26	138	G	3.6	190	51	2400	4900	140	3	0.3	4	51	18	0.9	218	1	<1	<1	<2	3	218.00	0.49	>109	
GG27	140	H	1.8	2900	63	2090	7600	300	<0.5	<0.1	<1	54	4	<0.4	107	2	<1	8	<2	<2	<2	53.50	0.28	>53
GG28	162	N	0.12	380	27	410	340	59	<0.5	<0.1	<1	29	<1	<0.4	20	<1	<1	6	<2	<2	<2	>20	1.21	>10
GG29	169	P	1.75	3314	55	900	3300	185	<0.5	<0.1	<1	31	4	1	58	3	6	12	2	3	5	19.33	0.27	29
GG30	186	L	2	4300	27	2345	8275	350	0.5	0.1	2	75	11	1.4	78	3	7	31	38	4	22	26.00	0.28	2
GG31	194	H	1.6	3300	55	912	3420	190	<0.5	<0.1	<1	23	2	<0.4	134	65	9	25	12	3	18	2.06	0.27	11
GG32	210	H	1.6	4200	47	3800	7420	310	1.9	0.3	2	102	3	<0.4	86	54	2	10	2	<2	<2	1.59	0.51	43
GG34	243	S	0.05	2300	58	22	1300	210	<0.5	<0.1	<1	39	<1	<0.4	<1	<1	<1	<1	<2	<2	<2	1.00	0.02	—
GG36	274	S	0.8	3300	40	272	1574	160	<0.5	0.2	2	74	1	0.5	<1	<1	<1	5	<2	<2	<2	1.00	0.17	—

Concentrations of sulfur are reported in wt.%, those of the PGE and Au, in ppb, and those of all others, in ppm. Symbols: D: depth, in meters, R: rock type: N: norite, L: lherzolite, P: pyroxenite, H: harzburgite, G: gabbro, S: serpentinized harzburgite. —: not established.

contents are revealed. The norite (<0.15 wt.% S) contains low Cu (22–290 ppm), Ni (121–340 ppm) and Co (29–52 ppm). The sulfide-bearing (3.2–3.9 wt.% S) gabbros contain higher Cu (2100–2400 ppm), Ni (4900–7600 ppm) and Co (130–320 ppm). The sulfide-bearing gabbro contains relatively higher As (3–5 ppm), Mo (3–4 ppm) and Sb (1.3–1.5 ppm) than all other rocks. A wide range of Cu:Ni values (0.18–0.85) is noted in norite samples, which could be attributed to randomly distributed chalcopyrite grains. The Cu:Ni values in the sulfide-bearing gabbros are lower and show a relatively narrow range (0.28–0.49) of variation.

The pyroxenite samples contain lower Cu (454–900 ppm), Ni (1141–3500 ppm) and Co (120–185 ppm) contents than those found in the sulfide-bearing gabbros. The Cu:Ni ratio in pyroxenite shows a narrow range of variation (0.19 to 0.4). The lowest Cu and Ni contents are detected in serpentinized harzburgite (22–272 ppm and 1300–1574 ppm, respectively). A relatively wide range of Cu and Ni abundances (900–3800 ppm and 3420–8275 ppm, respectively) characterizes harzburgite. The wide range of variation is reflected in the Cu:Ni values, which vary between 0.27 and 0.51.

#### *Platinum-group elements*

The PGE content of two samples of serpentinized harzburgite is generally below detection limit (1 ppb for Pd, Pt and Rh, and 2 ppb for Ir, Ru and Os). The Os content is below detection limit in both norite and sulfide-bearing gabbros. In all other rock units, the Os contents are near (up to 4 ppb) or below detection limit. The amount of Ru in sulfide-bearing gabbros and pyroxenite is near (3 and 5 ppb, respectively) or below the detection limit (2 ppb). Relatively high contents of Ru are detected in lherzolite (up to 22 ppb) and harzburgite (up to 18 ppb). The Ir contents are below the detection limit (2 ppb) in sulfide-bearing gabbros and close to detection limit in the pyroxenite. The Ir contents range from <2 to 12 ppb in harzburgite. The highest Ir content (38 ppb) is detected in lherzolite. The total IPGE (iridium subgroup of the PGE: Os + Ru + Ir) content in the rock units varies between 3 and 64 ppb. The low IPGE abundances in the Genina Gharbia rock types seem to be a general characteristic of the all Cu–Ni–PGE mineralization in the Eastern Desert [e.g., Abu Swayel: Helmy & Stumpfl (1995), Gabbro Akarem: Helmy & Mogessie (2001)].

The Rh contents range from <1 to 6 ppb in sulfide-bearing gabbros, from <1 to 8 ppb in pyroxenite, from <1 to 9 ppb in harzburgite, and from <1 to 7 ppb in lherzolite. Low Pt contents are detected in sulfide-bearing gabbros and pyroxenite (from <1 to 3 ppb). A wide range of variation in Pt contents characterizes harzburgite samples (2–65 ppb). Palladium is the most abundant PGE in the Genina Gharbia samples. The highest contents of Pd (210–226 ppb) are detected in the sul-

fide-bearing gabbros. The Pd contents range from <1 to 58 ppb in pyroxenite and from 8 to 86 ppb in lherzolite. The amount of Pd in harzburgite is relatively constant (average 108 ppb).

Similar contents of total PGE are detected in sulfide-bearing gabbro and harzburgite. The Pd:Pt ratio in samples in which both elements were detected varies from 75 to 218 (in sulfide-bearing gabbro) and from 1.6 to 53.5 in harzburgite. This ratio varies from <1 to 26 in lherzolite. The PPGE (palladium subgroup of the PGE: Pd + Pt + Rh):IPGE ratio decreases from 78.3 (one sample) in sulfide-bearing gabbro to 6.7 (one sample) in pyroxenite and increases again to 18.6 (average of five samples) in harzburgite and lherzolite.

#### PLATINUM-GROUP MINERALS AND ASSOCIATED PHASES

PGM and related minerals comprise the following phases: michenerite (PdBiTe), merenskyite (PdTe<sub>2</sub>), palladoan bismuthian melonite (NiTe<sub>2</sub>), hessite (Ag<sub>2</sub>Te), altaite (PbTe), tsumoite (BiTe), sylvanite (AuAgTe<sub>2</sub>), Au–Ag alloy and native tellurium. No Pt-dominant mineral has been identified. All these phases are documented from this deposit for the first time and occur in the sulfide-bearing gabbros in three distinctive textures: a) Fourteen grains occur as monomineralic inclusions and along cracks in sulfides, mainly pyrrhotite and pentlandite (Fig. 8A). b) Nine polymineralic grains are at the contact between sulfides and silicates (Fig. 8B). In this position, PGM and other tellurides exhibit euhedral crystal habits toward the sulfides, but irregular boundaries with the silicates. c) Forty-four grains are found as monomineralic and polymineralic inclusions in plagioclase and secondary silicates, *i.e.*, quartz, epidote, albite and actinolite (Figs. 8C, D, 9).

Palladoan bismuthian melonite (*e.g.*, Barkov *et al.* 2002) is the most abundant phase in the samples; it has been observed in the three different textures. It forms small (<30 μm) equant or elongate individual grains inside pyrrhotite and pentlandite (Fig. 8A). At the contact between sulfides and altered silicates, melonite is found as large (30–50 μm) grains commonly intergrown with hessite, michenerite, altaite and tsumoite. In this association, fine lamellae of the mineral have been observed in hessite. Where hosted in secondary silicates (mainly quartz and epidote), melonite forms anhedral grains of variable size (15 to 70 μm) associated with altaite and tsumoite. Electron-microprobe analyses of the mineral (Table 4) reveal variable Pd and Bi contents, ranging from 3.5 to 7.5 and from 2.5 to 8.5 wt.%, respectively. The high Pd and Bi contents are recorded in melonite hosted in secondary silicates. Also present are Fe (up to 1.6 wt.%), Ag (up to 1.8 wt.%) and S (up to 0.2 wt.%). The high contents of Fe, Ag and S are most probably due to contamination from the surrounding phases.

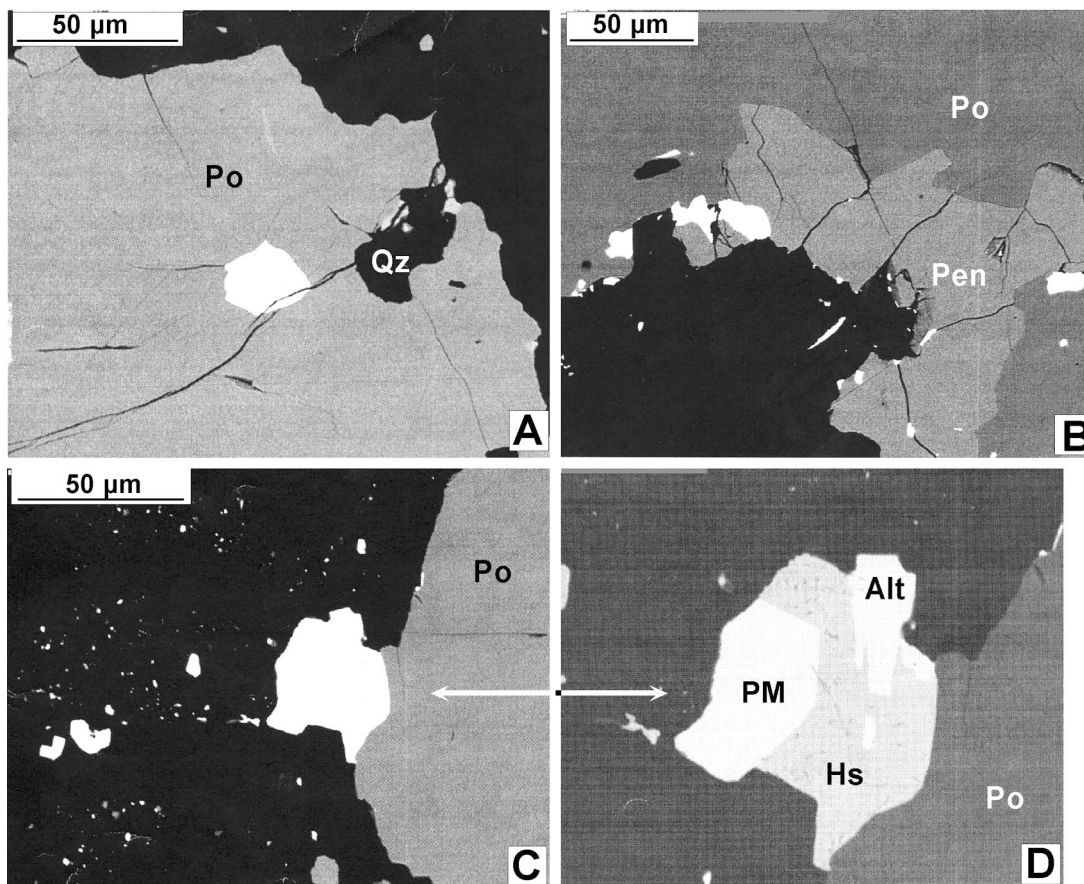


FIG. 8. Back-scattered images showing various textures of PGM from the sulfide-bearing gabbro. A) Pd-Bi-enriched melonite (white) included in pyrrhotite that hosts, and is surrounded by, quartz (Qz), sample GG25. B) PGM and other tellurides (white) form inclusions in, and at the interface of, pyrrhotite and pentlandite with secondary silicates (black), sample GG25. C) PGM and other tellurides entirely included in a secondary silicate matrix (black), sample GG26. D) The large white grain in C made of various tellurides; Pd-Bi melonite (PM), hessite (Hs) and altaite (Alt).

Michenerite was observed also in the above three textures; it forms small (<40 µm) anhedral crystals close to cracks in violarite, where it may be associated with native tellurium. At sulfide-silicate interfaces and in secondary silicates, michenerite forms composite grains with melonite, hessite and altaite (Figs. 9A, B). Electron-microprobe analyses of michenerite (Table 4) reveal a relatively wide range of Pd (29.1–32.1 wt.%), Te (36.8–43.6 wt.%) and Bi (39.5–43.6 wt.%) contents. Traces of Fe (up to 0.6 wt.%) and Ni (up to 0.8 wt.%) have been detected in michenerite. Unusually high Ag contents (up to 6.8 wt.%) have been measured in michenerite; these grains are not in direct contact with hessite, and so contamination is unlikely.

Merenskyite is usually present at the contact between pyrrhotite and silicates (mainly epidote). It forms small

(<30 µm) grains commonly associated with hessite. One anhedral grain (15 × 8 µm) was found inside hessite near a fracture in pyrrhotite. No traces of other PGE than Pd were detected in the merenskyite.

Hessite (10–70 µm) is widespread; about 100 grains were observed either at sulfide-silicate interfaces or as small inclusions in silicate groundmass. Very few grains of hessite were found near fractures in pyrrhotite. The large grains usually contain inclusions and blebs of melonite and altaite (Fig. 8D). Electron-microprobe data on hessite are listed in Table 3.

Altaite was observed in the two textures, *i.e.*, at the sulfide-silicate contacts and in secondary silicates, where it forms small (5–50 µm) individual or polyminerale grains. Altaite is usually associated with hessite, melonite and michenerite (Figs. 9A, B). Micro-

probe analyses of altaite show that it contains appreciable amounts of silver (up to 2.7 wt. %) and Bi (up to 0.5 wt. %). Relatively high levels of Fe (0.6–1.1 wt. %), Ni (0.1–0.8 wt. %) and Pd (0.1–0.6 wt. %) also are detected in altaite.

Tsumoite occurs at the margin of pyrrhotite grains associated with melonite, hessite and altaite. Small (<25  $\mu\text{m}$ ) grains of tsumoite are found in a quartz and epidote matrix close to sulfide patches in hornblende gabbro. Relatively high contents of Fe, Cu, Ag, and Ni (up to 1.25, 1.77, 2.11, and 0.16 at. %, respectively) were detected in tsumoite; contamination from the host cannot be excluded. One small grain (12  $\mu\text{m}$ ) of sylvanite was observed in association with michenerite and native tellurium, all as composite grains included in violarite.

Native Au–Ag alloy occurs as small (5–7  $\mu\text{m}$ ) grains dispersed in enstatite and actinolite. Its presence was

proved by semiquantitative electron-microprobe analysis.

Native tellurium fills thin fractures in violarite together with michenerite and sylvanite. Traces of Ag (up to 4.8 wt. %), Pb (up to 0.3 wt. %), Bi (up to 0.2 wt. %) and Pd (up to 0.14 wt. %) were detected.

#### DISCUSSION AND CONCLUSIONS

The systematic modal and compositional variations of rock-forming minerals at Genina Gharbia imply that the various rock types were derived from a common magma. It is widely accepted that decrease of Mg# in the ferromagnesian minerals as crystallization proceeds is characteristic of magmas undergoing fractional crystallization and accumulation. This inference is supported by previous geochemical studies (Khudier 1995). The dominance of hornblende, F-rich phlogopite, and fluo-

TABLE 4. REPRESENTATIVE COMPOSITIONS OF PGM AND ASSOCIATED PHASES, GENINA GHARBIA, EGYPT

Sample Mineral	GG25 Mch	GG24 Mch	GG26 Meh	GG25 Mln	GG26 Mln	GG26 Mln	GG25 Mrk	GG25 Alt	GG25 Hes	GG24 Tsm	GG25 N.Te
Bi wt%	42.22	41.92	42.14	7.15	6.58	6.16	12.81	0.24	0.14	51.91	0.24
Te	31.35	31.68	32.05	70.14	68.21	72.77	62.34	37.74	40.18	46.57	91.36
Pd	25.86	25.09	24.85	4.05	6.12	7.14	15.82	n.d.	n.d.	n.d.	0.14
Pt	n.d.	0.82									
Ag	n.d.	0.13	n.d.	1.52	1.81	n.d.	n.d.	0.15	60.01	0.61	3.49
Ni	0.13	0.19	0.11	14.47	13.63	14.01	7.65	0.86	n.d.	n.d.	1.02
Fe	0.21	0.32	0.26	0.93	1.59	0.31	n.d.	n.d.	n.d.	n.d.	0.95
Pb	n.d.	58.78	n.d.	n.d.	n.d.						
S	n.d.	0.17	n.d.	0.34							
Total	99.77	99.33	99.41	98.26	97.94	100.39	98.62	97.77	100.5	99.09	98.36

n.d. = not detected. Symbols: Mch: michenerite, Mln: Pd–Bi-enriched melonite, Mrk: merenskyite, Alt: altaite, Hes: hessite, Tsm: tsumoite, N.Te: native Te. Representative results of electron-microprobe analyses.

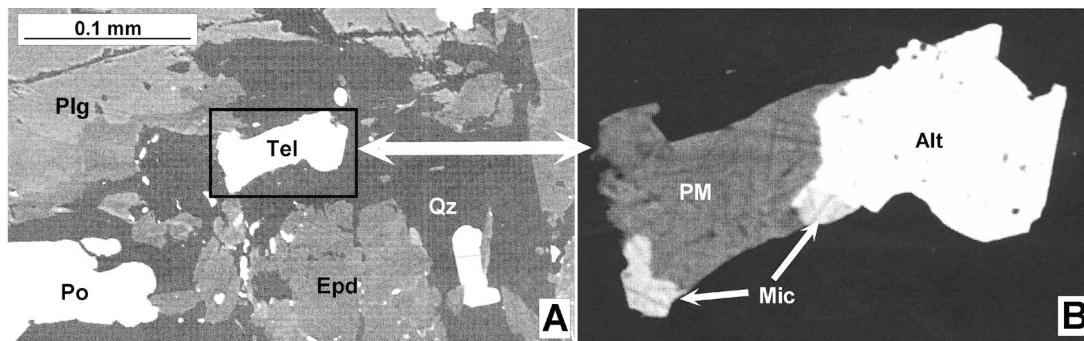


FIG. 9. A) A composite telluride grain hosted in quartz (Qz), surrounded by epidote (Epd) after plagioclase (Plg), sulfide-bearing gabbro, sample GG24. B) The composite grain in (A) made of altaite (Alt), Pd–Bi melonite (PM) and michenerite (Mic).

rapatite suggests that the magma was hydrous. Based on field and age relationships and geochemical studies, Helmy & El Mahhalwai (2003) suggest that the transport of H<sub>2</sub>O into the mantle below Gabbro Akarem and Genina Gharbia has taken place during subduction.

#### Mechanism of metal concentration and deposition

Base metals were precipitated as sulfides after the magma attained saturation. Sulfide saturation is attained either by the introduction of sulfur from crustal rocks (*e.g.*, Lambert *et al.* 1998) or simple fractionation processes (Keays 1995). The S/Se values (Table 3) of the harzburgite, lherzolite and norite are in the range of 2000–5000, typical of mantle-derived sulfides (Naldrett 1981). A mantle source is also indicated by the low As (normally <2 ppm) and Sb (<0.3 ppm) in these rocks. The sulfide-bearing gabbro, however, shows relatively high level of S (>3.6 wt.%) and lower S/Se values (*ca.* 2000), which may suggest input of S from the crust. This contrast can only be explained by different mechanisms of sulfide saturation: (1) at the early magmatic stage, saturation in sulfides was attained by fractionation; the gradual increase in S content from sulfide-poor mafic to ultramafic rocks (see Table 3) support this inference. (2) At the late magmatic stage, additional S was introduced from a crustal source, as is supported by the relatively high As, Mo and Sb in the sulfide-bearing gabbro (Barnes & Thériault 1998; see also below).

At the early magmatic stage, the precipitation of base and precious metals as sulfides is indicated in the S-metal variation diagrams (Fig. 10). The norite, pyroxenite, lherzolite and harzburgite define a fractionation trend on the S *versus* Ni, Cu and Co diagrams. On the S and Cu *versus* total PGE contents (Fig. 11), similar trends are observed for these rocks. The increase of Pd/Ir value from 18 (average of five samples) in harzburgite to 33 (one sample) in pyroxenite also is consistent with the fractionation trend. The positive correlations of S and Cu with total PGE imply that PGE at this stage were concentrated by sulfides. It is widely accepted that immiscible base-metal-enriched sulfide liquid acts as a collector for PGE in magmatic systems (Barnes *et al.* 1985).

An important mineralogical observation at Genina Gharbia is the absence of any PGM in the network sulfides hosted in the ultramafic rocks. These rocks contain PGE contents similar to the PGM-bearing mineralized gabbro. The PGE are likely to be hosted in the base-metal sulfides. It is widely accepted that all PGEs were originally part of a magmatic monosulfide solid-solution (*mss*) (Ballhaus & Ryan 1995). Although the high Pd and Pt contents in cobaltite could be due to sub-microscopic blebs (as indicated by microscopic investigation), the occurrence of these blebs themselves supports the suggestion that some PGE were dissolved in sulfides and sulfarsenides. Platinum and Pd show a positive correlation with Co in the harzburgite and

lherzolite (Fig. 12), which suggests that these metals are incorporated in pentlandite and cobaltite. Recently, the quantitative determination (ppm range) of PGE in common sulfides became possible. Sharara *et al.* (1999) reported high Pd values (1030 ppb) in pentlandite from Gabbro Akarem, a deposit similar to Genina Gharbia, in the Eastern Desert. The published data confirm that some of the PGE, Pt and Pd in particular, may reach significant concentrations in pentlandite and cobaltite–gersdorffite, for example (Cabri 1992, Gervilla & Kojonen 2002, Oberthür *et al.* 2003). Barkov *et al.* (1999) concluded that PGE substitute for Co in the cobaltite–gersdorffite series. Experimentally, Makovicky *et al.* (1986) have shown that several percent Pd may dissolve in Fe–Ni sulfides.

On the S-metal variation diagrams (Figs. 10, 11) the sulfide-bearing gabbro shows a distinct distribution of metals relative to the other rock types. This anomalous

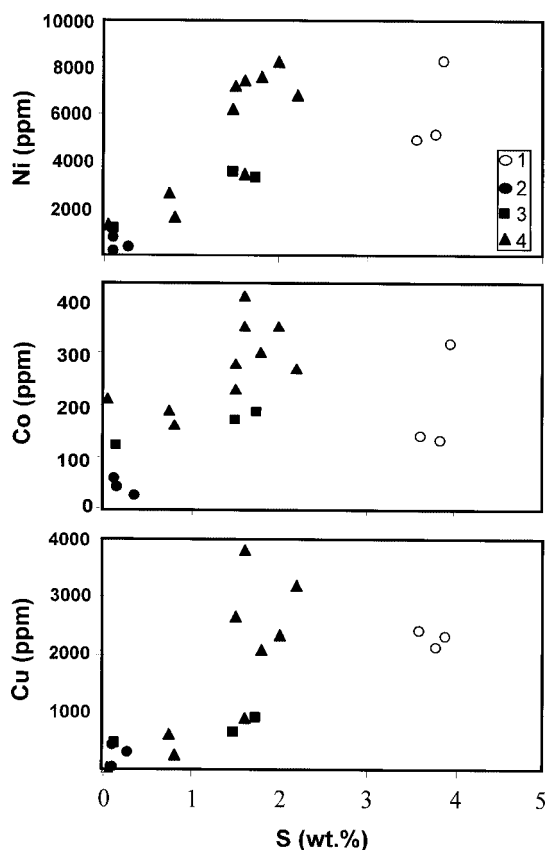


FIG. 10. Sulfur–metal variation diagrams for samples from drill core DH4, Genina Gharbia. Symbols: 1: sulfide-bearing gabbro, 2: norite, 3: pyroxenite, and 4: harzburgite and lherzolite.

behavior suggests a different mechanism of metal concentration. As shown in the mineralogy section, 77% of grains of PGM and other tellurides are hosted in altered silicates. At this stage, the PGE were likely to have been concentrated by late-magmatic volatile-rich fluids. This inference is supported by the high Pd/Pt value in sulfide-bearing gabbro relative to the other rocks. As shown in the geochemistry section, the sulfide-bearing gabbro shows low contents of Cr, Ni and Co. This feature demonstrates that the magma was relatively evolved. Therefore, I suggest that the dominance of Pd over Pt in the sulfide-bearing gabbro is attributed to the relatively evolved nature of the magma. Highly evolved magmas are characterized by high Pd/Pt values (*e.g.*, Geordie Lake Intrusion, Coldwell Complex, Ontario; Mulja & Mitchell 1990). Concentration of Pd, Pt and Rh in late magmatic fluids was suggested for many well-known PGE deposits, *e.g.*, the Bushveld Igneous Complex (Ballhaus & Stumpfl 1986), the Duluth complex, Minnesota (Mogessie *et al.* 1991) and the North Range of the Sudbury Igneous Complex (Farrow & Watkinson 1992). The high Cl-contents of hydrous silicates, chlorapatite and fluorapatite and the type of alteration observed at Genina Gharbia suggest that these metals were transported as chloride complexes.

The common association of Pd bismuthotellurides with Ni, Ag, Pb, Bi and Au tellurides in the sulfide-bearing gabbro suggests that the fluids were also rich in Te, Bi and other precious metals. Paktunc *et al.* (1990) concluded that the availability of Bi and Te effectively con-

trols the extent of PGE solution in sulfide hosts. The availability of Te and Bi in a late-magmatic volatile-rich fluid led to the deposition of PGE as discrete PGM phases. The absence (or low contents) of Te and Bi at the early magmatic stage explains the absence of PGM in the network sulfides hosted in harzburgite and lherzolite despite their high PGE content.

In a recent investigation of the Bushveld Complex, Cawthorn *et al.* (2002) discussed the relationship between PGE and PGM. The authors showed that there is a dichotomy between the constancy of PGE and the variability of PGM. The authors attributed the concentration of PGE to a primary first-order process and the evolution of PGM to secondary processes. These secondary processes are controlled by cooling, local changes in  $f(S_2)$  and subsolidus re-equilibration. The mineralogical and geochemical data presented here for the Genina Gharbia are consistent with their conclusion. In addition to the factors suggested to be controlling these secondary processes, we add the availability of semimetals, like Te and Bi, as a factor controlling PGM deposition.

Later, and during faulting and shearing, base-metal sulfides were fractured and mobilized, to be concentrated along shear zones in the harzburgite. The role of tectonics is strongly indicated by the location of the Cu-Ni mineralization in the highly tectonized part of the area.

#### The role and source of fluids

Many of the petrographic and mineralogical observations described from Genina Gharbia have been docu-

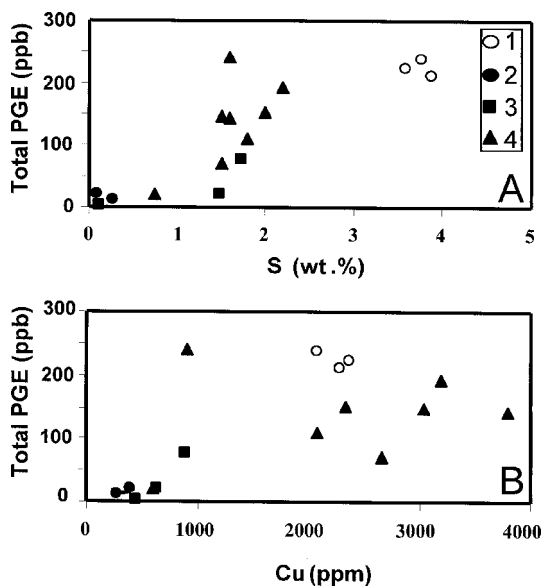


FIG. 11. Plot of S (A) and Cu (B) versus total PGE contents, for samples from drill core DH4. Symbols as in Figure 10.

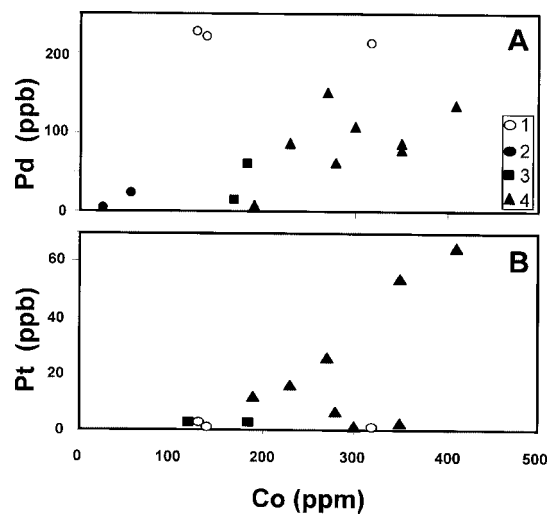


FIG. 12. Concentrations of Co versus Pd (A) and Pt (B) for samples from drill core DH4. Symbols as in Figure 10.

mented in similar deposits [Two Duck Lake gabbro: Good & Crocket (1994), Partridge River intrusion: Watkinson & Ohnenstetter (1992), and Duluth Complex: Mogessie *et al.* (1991)]. The important role played by fluids in the genesis of these deposits is widely accepted. These fluids may have (1) carried all compounds with high fluid/melt partition coefficients, as well as metals capable of forming OH- and Cl-complexes (Ballhaus & Stumpfl 1986). In this case, the PGE are assumed to have fractionated into the Cl-rich fluid as Cl-complexes rather than being dissolved in the sulfide melt, and migrated over short distances (Good & Crocket 1994), or (2) interacted with the magmatic assemblage (sulfides and silicates) to dissolve PGE and form the telluride and secondary silicate assemblages (Watkinson & Ohnenstetter 1992). In this case, these fluids could cause extensive alteration of the host rocks.

To know which effect was working at Genina Gharbia, we refer to the textures of PGM. As stated in the mineralogy section, 23% of the PGM grains are located close to the margins of pyrrhotite, and 77% of the grains are either hosted in secondary silicates or at the contact between sulfides and silicates. At the sulfide–silicate interface, PGM grains show euhedral habits against sulfides but irregular boundaries with silicates. PGM inclusions in pyrrhotite are easily understood through extraction from the sulfide melt. This mechanism was of minor importance, as indicated by the low population of PGM grains included in sulfides. The PGM at the contact between sulfides and silicates could be the result of PGE precipitation around the periphery of droplets of sulfide melt due to cooling of the fluids carrying them (Ballhaus & Stumpfl 1986) or crystallization of PGE from a liquid sulfide trapped within a solid silicate matrix (Vermaak & Hendriks 1976). The latter mechanism means that these phases had crystallized prior to the sulfides. In both scenarios, the PGM are unlikely to be the result of fluid–sulfide reaction. Therefore, I conclude that at Genina Gharbia, the late-magmatic volatile-rich fluids carried the base and precious metals and interacted with the early-formed silicates to deposit PGM and to form the secondary silicates. The observed petrographic features reflect reactions that occur as the temperature decreased and the fluid evolved. Although no microthermometry studies have been made on Genina Gharbia samples, a temperature range of 340–175°C was calculated by Farrow & Watkinson (1992) from fluid inclusions hosted in quartz associated with a similar assemblage of alteration minerals.

There are two possible sources for such fluids: (1) the mafic magma itself, (2) an external source (from metasedimentary rocks) or a mixture of (1) and (2). An important petrological feature of the ultramafic units at Genina Gharbia is the high content of primary hydrous silicates (magnesiophorite and phlogopite) and fluorapatite, which indicates a hydrous parental magma. It is likely that the hydrothermal fluid appeared during

fractionation and differentiation of the hydrous magma. The crystallization of early anhydrous minerals from a volatile-saturated liquid will result in separation of a volatile-rich fluid, which exsolves from the solidifying interstitial liquid (Boorman *et al.* 2003).

Such a fluid phase also could have been introduced from the surrounding metasedimentary rocks. The restriction of the PGM to those parts that show the strongest evidence of deformation and quartz veining is a good indication. The occurrence of quartz in the alteration assemblage and the presence of Ni and Co arsenides and molybdenite also support this inference. The occurrence of molybdenite in the basal zone of Duluth Complex led Mogessie *et al.* (1992) to suggest the involvement of fluids from the nearby metasedimentary Virginia Formation. This inference was supported by isotopic studies of the basal zone of Duluth Complex (Ripley & Al Jasar 1987) and other areas (*e.g.*, Voisey's Bay Ni–Cu–Co deposit: Ripley *et al.* 1999). The mechanisms by which such fluids could have been introduced include: a) early incorporation of inclusions of metasedimentary rocks in the magma (*e.g.*, Gervilla *et al.* 1997, Sproule *et al.* 1999), b) direct input from the metasedimentary rocks in contact with the Genina Gharbia intrusion, and c) transfer of fluids and vapor from the metasedimentary rocks along faults and fractures. The absence of metasedimentary xenoliths in the intrusion and the occurrence of the Cu–Ni–PGE mineralization in the highly faulted and fractured part near the metasedimentary rocks support (b) and (c) above. However, the dominance of enstatite in the various units may also support (a) above. Whole-rock geochemistry and stable isotope studies are needed to evaluate the role of sedimentary components in the hydrothermal history of the Genina Gharbia mineralization.

#### *Genetic model*

According to the host rock, mode of occurrence and associated mineral phases, a three-stage process is proposed to account for the different types of sulfides.

Stage (1): When the ultramafic magma attained saturation in sulfides due to fractionation, a sulfide liquid was formed. Sulfides were precipitated as a network between early-formed olivine and pyroxenes. All PGE were incorporated in sulfides and sulfarsenides, pentlandite and cobaltite–gersdorffite, in particular.

Stage (2): After fractionation of the magma, additional sulfur and other semimetals were introduced from the surrounding metasediments. Both base and precious metals were separated and concentrated in the highly evolved H<sub>2</sub>O-enriched fluid formed in equilibrium with gabbroic magma. Sulfides, platinum-group minerals and other tellurides crystallized from this metal-rich fluid at lower temperature. The fluid formed the phlogopite, chlorapatite and fluorapatite, and later interacted with the early-formed silicates to form the secondary, low-

temperature phases like actinolite, epidote, albite and quartz.

Stage (3): There followed local, short-distance mobilization and recrystallization of sulfides due to post-magmatic faulting and shearing.

#### Type of mineralization

The Genina Gharbia is intruded along one of the deep faults intersecting the Eastern Desert in an east-northeasterly direction (Garson & Shalaby 1976). The concentric zoning showed by the intrusion is similar to that in Cretaceous Alaskan-type complexes (Irvine 1974). A similar intrusion (Gabbro Akarem) was recently described as a late Precambrian analogue of Alaskan-type complexes (Helmy & El Mahhalwai 2003). The Genina Gharbia intrusion shows many petrographic features, specially the dominance of orthopyroxene, in common with Alaskan-type complexes. Although described from two Alaskan-type complexes [Salt Chuck: Loney & Himmelberg (1992), and Gabbro Akarem: Helmy & Mogessie (2001)], the occurrence of Cu–Ni–PGE mineralization in Alaskan-type complexes is not common. There are many striking mineralogical similarities (especially in the sulfide-bearing hornblende gabbro) between Genina Gharbia and the Two Duck Lake gabbro, the Partridge River intrusion (Duluth

Complex), the Marathon Cu–Ni–PGE deposit, the Geordie Lake Gabbro, Coldwell Complex, Ontario. However the Cu–Ni–PGE mineralization of these complexes are mainly hosted in gabbroic rocks, which form separate intrusions not related to layered complexes. In these deposits, the common mineralogical similarities were attributed to late-magmatic fluids concentrating and depositing the base and precious metals. As discussed above, the role of hydrothermal fluid is more evident in the sulfide-bearing gabbro. The similarity between Genina Gharbia and these deposits thus only pertains to the late-magmatic history. The fact that the Genina Gharbia intrusion is made of a sequence of mafic–ultramafic rocks makes it more similar to layered intrusions. The sulfide mineralogy (pentlandite > chalcocopyrite) of Genina Gharbia and the rock assemblage (ultramafic–mafic) make the deposit similar to the classic magmatic sulfide deposits (Naldrett 1989). For comparison, chondrite-normalized PGE patterns for the Genina Gharbia rocks (recalculated to 100% sulfides assuming 38% S in the sulfide liquid) and PGE-mineralized magmatic bodies are illustrated in Figure 13. The sulfide-bearing gabbro has a very similar pattern to the Stillwater complex. Although relatively enriched in IPGE, the pyroxenite and harzburgite have also similar patterns to the Stillwater complex.

#### ACKNOWLEDGEMENTS

Prof. Georg Hoinkes, Institute of Mineralogy and Petrology, Karl Franzens University, Graz, Austria is thanked for the analytical facilities offered. Editorial handling and critical comments by Robert F. Martin are greatly acknowledged. F. Zaccarini and an anonymous reviewer are thanked for their helpful comments.

#### REFERENCES

- BALLHAUS, C. & RYAN, C.G. (1995): Platinum-group elements in the Merensky Reef. 1. PGE in solid solution in base metal sulfides and the down-temperature equilibration history of Merensky ores. *Contrib. Mineral. Petrol.* **122**, 241–251.
- \_\_\_\_\_ & STUMPFEL, E.F. (1986): Sulfide and platinum mineralization in the Merensky Reef: evidence from hydrous silicates and fluid inclusion. *Contrib. Mineral. Petrol.* **94**, 193–204.
- BARKOV, A.Y., LAFLAMME, J.H.G., CABRI, L.J. & MARTIN, R.F. (2002): Platinum-group minerals from the Welgreen Ni–Cu–PGE deposit, Yukon, Canada. *Can. Mineral.* **40**, 651–669.
- \_\_\_\_\_, THIBAUT, Y., LAAJOKI, K.V.O., MELEZHNIK, V.A. & NILSSON, L.P. (1999): Zoning and substitutions in Co–Ni–(Fe)–PGE sulfarsenides from the Mount General'skaya layered intrusion, Arctic Russia. *Can. Mineral.* **37**, 127–142.

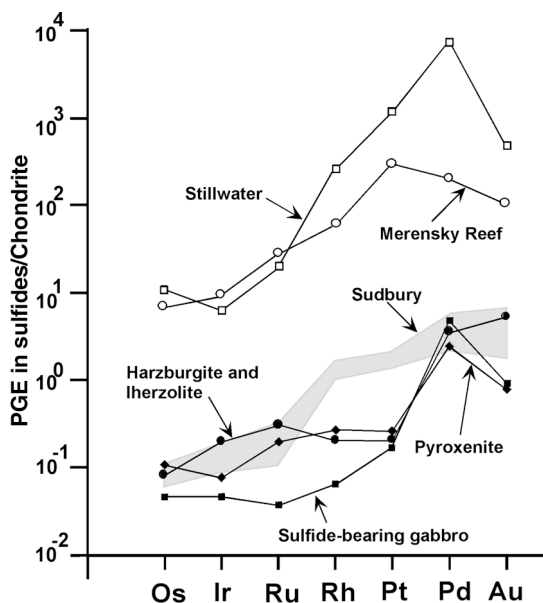


FIG. 13. Chondrite-normalized PGE patterns of Genina Gharbia mineralized rocks (recalculated to 100% sulfides). The PGE patterns of Stillwater complex, Merensky Reef, and Sudbury are shown for comparison. The data are from Naldrett (1981).

- BARNES, S.J., NALDRETT, A.J. & GORTON, M.P. (1985): The origin of the fractionation of platinum-group elements in terrestrial magmas. *Chem. Geol.* **53**, 303-323.
- BARNES, S.-J. & THÉRIAULT, R.D. (1998): The influence of assimilation and cooling rate on the composition of magmatic sulfides: examples from the Muskox and Duluth intrusions. *Eighth Int. Platinum Symp. (South Africa)*, 29 (abstr.).
- BOORMAN, S.L., MCGUIRE, J.B., BOUDREAU, A.E. & KRUGER, F.J. (2003): Fluid overpressure in layered intrusions: formation of a breccia pipe in the Eastern Bushveld Complex, Republic of South Africa. *Mineral. Deposita* **38**, 356-396.
- BUGROV, V.A. (1974): On the geological operations carried out from June 1972 to June 1974. *U.N. Development Program, Tech. Rep.*
- CABRI, L.J. (1992): The distribution of trace precious metals in minerals and mineral products. *Mineral. Mag.* **56**, 289-308.
- CAWTHORN, R.G., LEE, C.A., SCHOUWSTRA, R.P. & MELLOW-SHIP, P. (2002): Relationship between PGE and PGM in the Bushveld Complex. *Can. Mineral.* **40**, 311-328.
- EL GABY, S., LIST, F. K. & TEHRANI, R. (1990): The basement complex of the Eastern Desert and Sinai. In *The Geology of Egypt* (R. Said, ed.). A.A. Balkema, Rotterdam, The Netherlands (175-199).
- EL MAHALLAWI, M.M. (1996): Geochemistry and petrogenesis of the gabbroic rocks at Genina Gharbia, south Eastern Desert, Egypt. *Egypt. J. Geol.* **40**, 587-603.
- FARROW, C.F.G. & WATKINSON, D.H. (1992): Alteration and the role of fluids in Ni, Cu, and platinum-group element deposition, Sudbury Igneous Complex Contact, Onaping-Levack area, Ontario. *Mineral. Petrol.* **46**, 67-83.
- FREDRICKSSON, G. (1974): On the geology and mineralogy at Genina Gharbia, Eastern Desert, Egypt. Project Report.
- GARSON, M.S. & SHALABY, I.M. (1976): Precambrian – Lower Paleozoic plate tectonics and metallogenesis in the Red Sea region. *Geol. Assoc. Can., Spec. Pap.* **14**, 573-596.
- GERVILLA, F. & KOJONEN, K. (2002): The platinum-group minerals in the upper section of the Keivitsansarvi Ni–Cu–PGE deposit, northern Finland. *Can. Mineral.* **40**, 377-394.
- \_\_\_\_\_, SANCHEZ-ANGUITA, A., ACEVEDO, R.D., FENOLL HACH-ALÍ, P. & PANIAGUA, A. (1997): Platinum-group element sulpharsenides and Pd bismuthotellurides in the metamorphosed Ni–Cu deposit at Las Aguilas (Province of San Luis, Argentina). *Mineral. Mag.* **61**, 861-877.
- GOOD, D.J. & CROCKET, J.H. (1994): Genesis of the Marathon Cu – platinum-group element deposit, Port Coldwell alkaline complex, Ontario: a mid-continent rift-related magmatic sulfide deposit. *Econ. Geol.* **89**, 131-149.
- GUILLOIN, J.C. (1974): Geophysical survey of Genina Gharbia. Project Report.
- HELMY, H.M. & EL MAHALLAWI, M.M. (2003): Gabbro Akarem mafic-ultramafic complex, Eastern Desert, Egypt: a Late Precambrian analogue of Alaskan-type complexes. *Mineral. Petrol.* **77**, 85-108.
- \_\_\_\_\_, & MOGESSIE, A. (2001): Gabbro Akarem, Eastern Desert, Egypt: Cu–Ni–PGE mineralization in a concentrically zoned mafic ultramafic complex. *Mineral. Deposita* **36**, 58-71.
- \_\_\_\_\_, & STUMPFL, E.F. (1995): Genesis of the Abu Swayel Cu–Ni–PGE mineralization, South Eastern Desert, Egypt. In *Mineral Deposits from their Origin to their Environmental Impacts* (J. Pašava, B. Kribek & K. Zak, eds.). Proc. Third Biennial SGA Meeting (Prague), 117-120.
- \_\_\_\_\_, & KAMEL, O.A. (1995): Platinum-group minerals from the metamorphosed Abu Swayel Cu–Ni–PGE deposit, South Eastern Desert, Egypt. *Econ. Geol.* **90**, 2350-2360.
- IRVINE, T.N. (1974): Petrology of the Duke Island ultramafic complex, southeastern Alaska. *Geol. Soc. Am., Mem.* **138**.
- KAMEL, O.A., GAD, M.A. & MISSACK, E.A. (1990): The Cu–Ni mineralization in El Genina El Gharbia, Eastern Desert, Egypt. *Proc. Egypt. Acad. Sci.* **40**, 195-209.
- KEAYS, R.R. (1995): The role of komatiitic and picritic magmatism and S-saturation in the formation of ore deposits. *Lithos* **34**, 1-18.
- KHUDIER, A.A. (1995): El-Genina El-Gharbia and El-Genina El-Sharkia ultramafic-mafic intrusions, Eastern Desert, Egypt: geology, petrology, geochemistry and petrogenesis. *Bull. Fac. Sci. Assiut Univ.* **24**, 177-219.
- LAMBERT, D.D., FOSTER, J.G., FRICK, L.R., RIPLEY, E.M. & ZIENTEK, M.L. (1998): Geodynamics of magmatic Cu–Ni–PGE sulfide deposits: new insights from the Re–Os isotopic system. *Econ. Geol.* **93**, 121-136.
- LONEY, R.A. & HIMMELBERG, G.R. (1992): Petrogenesis of the Pd-rich intrusion at Salt Chuck, Prince of Wales Island: an early Paleozoic Alaskan-type ultramafic body. *Can. Mineral.* **30**, 1005-1022.
- MAKOVICKY, M., MAKOVICKY, E. & ROSE-HANSEN, J. (1986): Experimental studies on the solubility and distribution of platinum-group elements in base metal sulfides in platinum deposits. In *Metallogeny of Basic and Ultrabasic Rocks* (M.J. Gallagher, R.A. Ixer, C.R. Neary & H.M. Prichard, eds.). The Institution of Mining and Metallurgy, London, U.K. (415-425).
- MISSACK, E.A. (1981): *Mineralogy and Geochemistry of the Cu–Ni Mineralization of Genina Gharbia, Eastern Desert, Egypt*. M.Sc. thesis, Minia Univ., Minia, Egypt.
- MOGESSIE, A., KUCHA, H. & STUMPFL, E.F. (1992): Occurrence of molybdenite in the basal zone of the Duluth Complex, Minnesota, USA. *Neues Jahrb. Mineral., Monatsh.*, 433-440.

- \_\_\_\_\_, STUMPFEL, E.F. & WEIBLEN, P.W. (1991): The role of fluids in the formation of platinum-group minerals, Duluth Complex, Minnesota: mineralogic, textural, and chemical evidence. *Econ. Geol.* **86**, 1506-1518.
- MULJA, T. & MITCHELL, R.H. (1990): Platinum-group minerals and tellurides from the Geordie Lake Intrusion, Coldwell Complex, northwestern Ontario. *Can. Mineral.* **28**, 489-501.
- NALDRETT, A.J. (1981): Nickel sulfide deposits: classification, composition, and genesis. *Econ. Geol., 75th Anniv. Vol.*, 628-685.
- \_\_\_\_\_. (1989): *Magmatic Sulfide Deposits*. Clarendon Press, New York, N.Y.
- OBERTHÜR, T., WEISER, T.W., GAST, L. & KOJONEN, K. (2003): Geochemistry and mineralogy of platinum-group elements at Hartley platinum mine, Zimbabwe. 1. Primary distribution patterns in pristine ores of the Main Sulfide Zone of the Great Dyke. *Mineral. Deposita* **38**, 327-343.
- PAKTUNC, A.D., HULBERT, L.J. & HARRIS, D.C. (1990): Partitioning of the platinum-group and other trace elements in sulfides from the Bushveld complex and Canadian occurrences of nickel-copper sulfides. *Can. Mineral.* **28**, 475-488.
- RIPLEY, E.M. & AL-JASAR, T.J. (1987): Sulfur and oxygen isotope studies of melt - country rock interaction, Babbit Cu-Ni deposit, Duluth Complex. *Econ. Geol.* **82**, 87-107.
- \_\_\_\_\_, PARK, YOUNG-ROK, LI, CHUSI & NALDRETT, A.J. (1999): Sulfur and oxygen isotopic evidence on country rock contamination in the Voisey's Bay Ni-Cu-Co deposit, Labrador, Canada. *Lithos* **47**, 53-68.
- SHARARA, N.A., WILSON, G.C. & RUCKLIDGE, J.C. (1999): Platinum-group elements and gold in Cu-Ni-mineralized peridotite at Gabbro Akarem, Eastern Desert, Egypt. *Can. Mineral.* **37**, 1081-1097.
- SPROULE, R.A., LAMBERT, D.D. & HOATSON, D.M. (1999): Re-Os isotopic constraints on the genesis of the Sally Malay Ni-Cu-Co deposit, East Kimberley, Western Australia. *Lithos* **47**, 89-106.
- TAKLA, M.A. & NOWEIR, A.M. (1980): Mineralogy and mineral chemistry of the ultramafic mass of El Rubshi, Eastern Desert, Egypt. *Neues Jahrb. Mineral., Abh.* **140**, 17-28.
- VERMAAK, C.F. & HENDRIKS, L.P. (1976): A review of the mineralogy of the Merensky Reef, with specific reference to new data on the precious metal mineralogy. *Econ. Geol.* **71**, 1244-1269.
- WATKINSON, D.H. & OHNENSTETTER, D. (1992): Hydrothermal origin of platinum-group mineralization in the Two Duck Lake intrusion, Coldwell Complex, northwestern Ontario. *Can. Mineral.* **30**, 121-136.

Received June 15, 2003, revised manuscript accepted January 15, 2004.